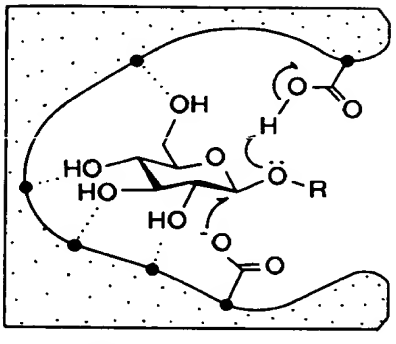


ground state binding
[E–S]

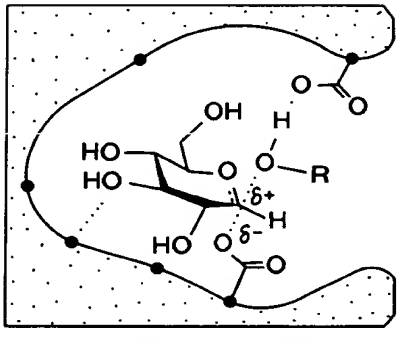


transition state binding
[E–S] ‡
R = aglycon residue

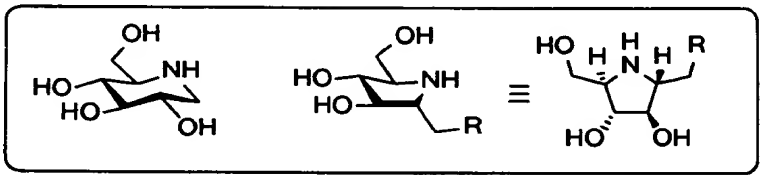


FIG. 1

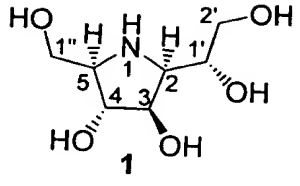


1

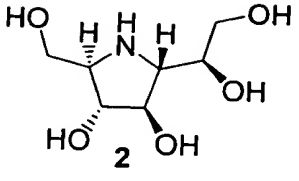


2

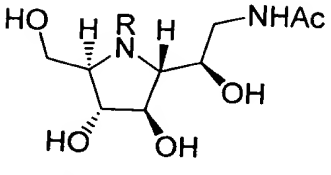


**6** R = H
**7** R = $CH_3$
**8** R = $CH_2CH_3$

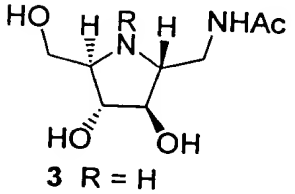


**3** R = H
**4** R = $CH_3$
**5** R = $(CH_2)_3CH_3$

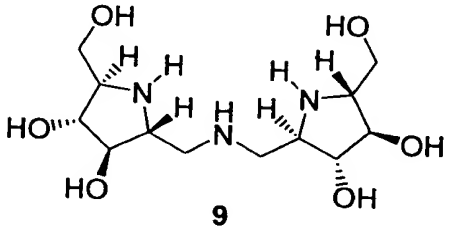


**9**

FIG. 2

| | $K_i$ ($\mu$M) | | | | |
|---|---|---|---|---|---|
| | α-glucosidase[a] | β-glucosidase[b] | β-*N*-acetylglucosaminidase | β-*N*-acetylhexosaminidase | |
| compd | *Saccaromyces sp* | sweet almond | bovine kidney[c] | human placenta A[d] | p[e] |
| 1[f] | 330 | 50 | -[h] | - | - |
| 2[f] | 28 | 2.6 | - | - | - |
| 3 | 380 | *[g] | $2.9 \times 10^{-1}$ | $2.2 \times 10^{-1}$ | $2.6 \times 10^{-1}$ |
| 4 | ni | ni | $1.1 \times 10^{-1}$ | $1.4 \times 10^{-1}$ | $8.0 \times 10^{-2}$ |
| 5 | ni | ni | 1.3 | $5.1 \times 10^{-1}$ | $2.4 \times 10^{-1}$ |
| 6 | * | 2.2 | * | - | - |
| 7 | * | 45 | * | - | - |
| 8 | ni | 120 | ni[i] | - | - |
| 9 | 53 | 37 | - | - | - |

[a] $K_m$ = 0.30 mM, $V_{max}$ = 0.7 ($\mu$M/s)/mg. [b] $K_m$ = 3.2 mM, $V_{max}$ = 3.2 ($\mu$M/s)/mg. [c] $K_m$ = 4.1 mM, $V_{max}$ = 6.4 ($\mu$M/s)/mg. [d] $K_m$ = 2.5 mM, $V_{max}$ = 2.1 ($\mu$M/s)/mg. [e] $K_m$ = 2.8 mM, $V_{max}$ = 2.3 ($\mu$M/s)/mg. [f] Preliminary assay result using photometric assay gave $K_i$ values: 430 and 18 $\mu$M for compound 1 and 7.2 and 7.6 $\mu$M for compound 2 toward α-glucosidase and β-glucosidase, respectively. See also refs 6a and 19. [g] *: poor inhibitor with $IC_{50}$ above 0.5 mM. [h] -: not tested. [i] ni: not inhibitor.

FIG. 3

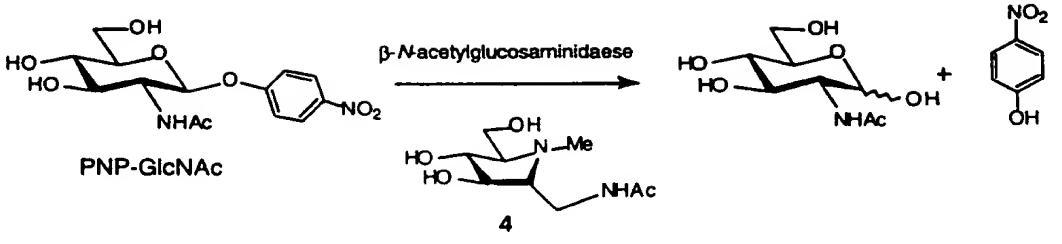


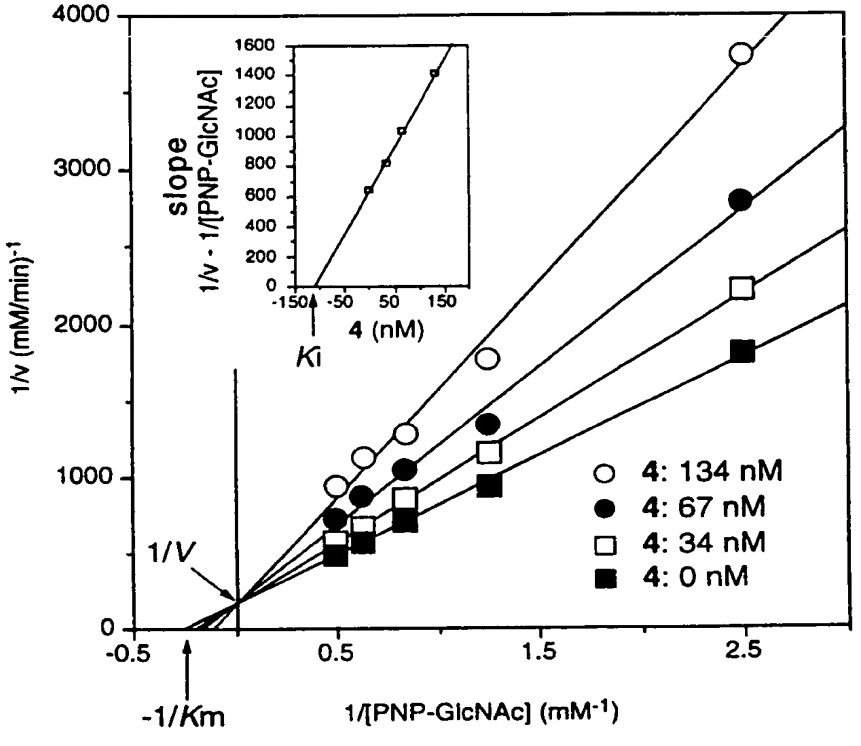


FIG. 4

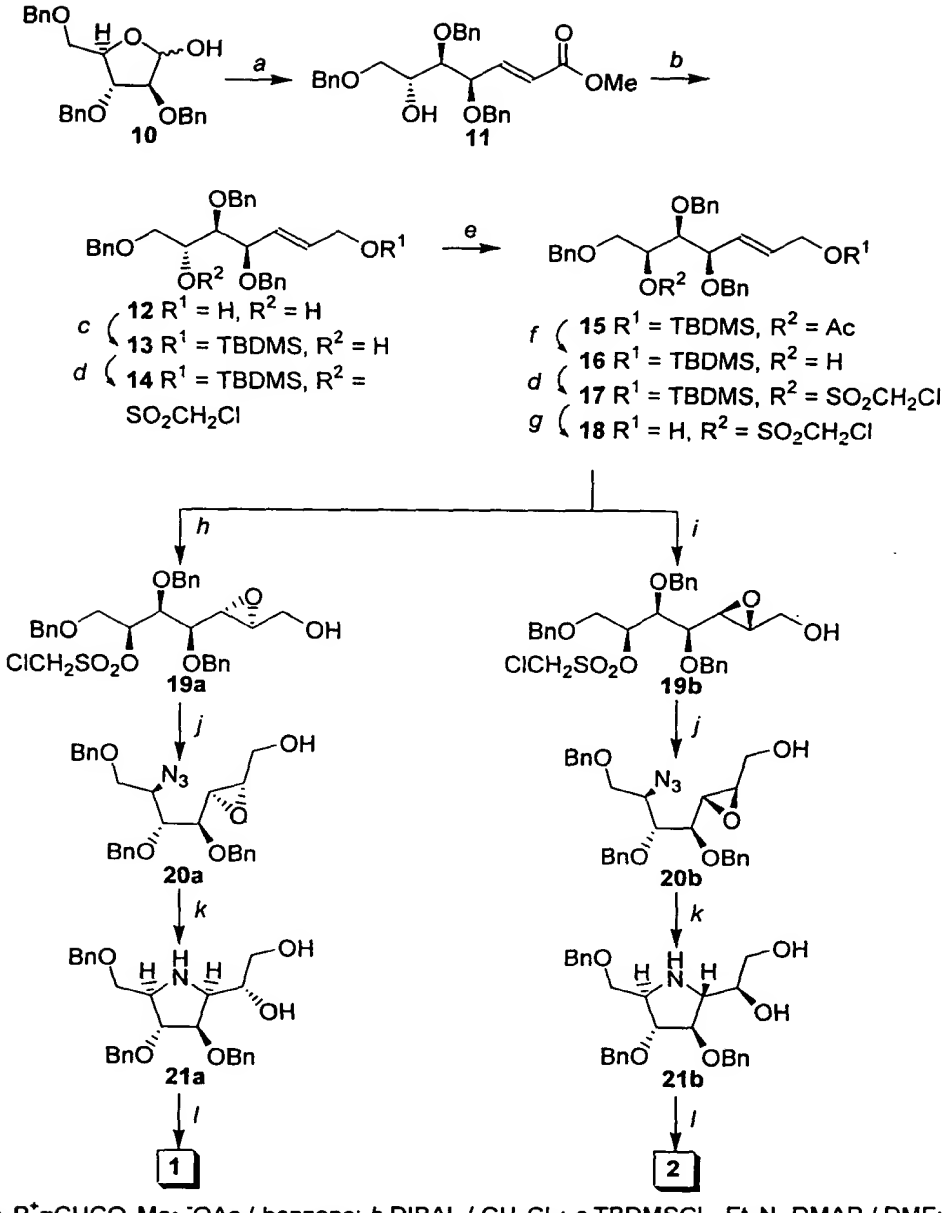


*a* $Ph_3P^+$=$CHCO_2Me$ $^-OAc$ / benzene; *b* DIBAL / $CH_2Cl_2$; *c* TBDMSCl - $Et_3N$ -DMAP / DMF; *d* $ClCH_2SO_2Cl$ - Pyr.; *e* CsOAc - 18-crown-6 / toluene; *f* NaOMe; *g* 1N-HCl / THF; *h* *t*-BuOOH - Ti(O-*i*-Pr)$_4$ - L-(+)-diethyltartrate - MS 4A / $CH_2Cl_2$; *i* *t*-BuOOH - Ti(O-*i*-Pr)$_4$ - D-(-)-diethyltartrate - MS 4A / $CH_2Cl_2$; *j* $NaN_3$ / DMF; *k* $Ph_3P$ / THF; *l* $H_2$ - Pd/C / MeOH.

FIG. 5

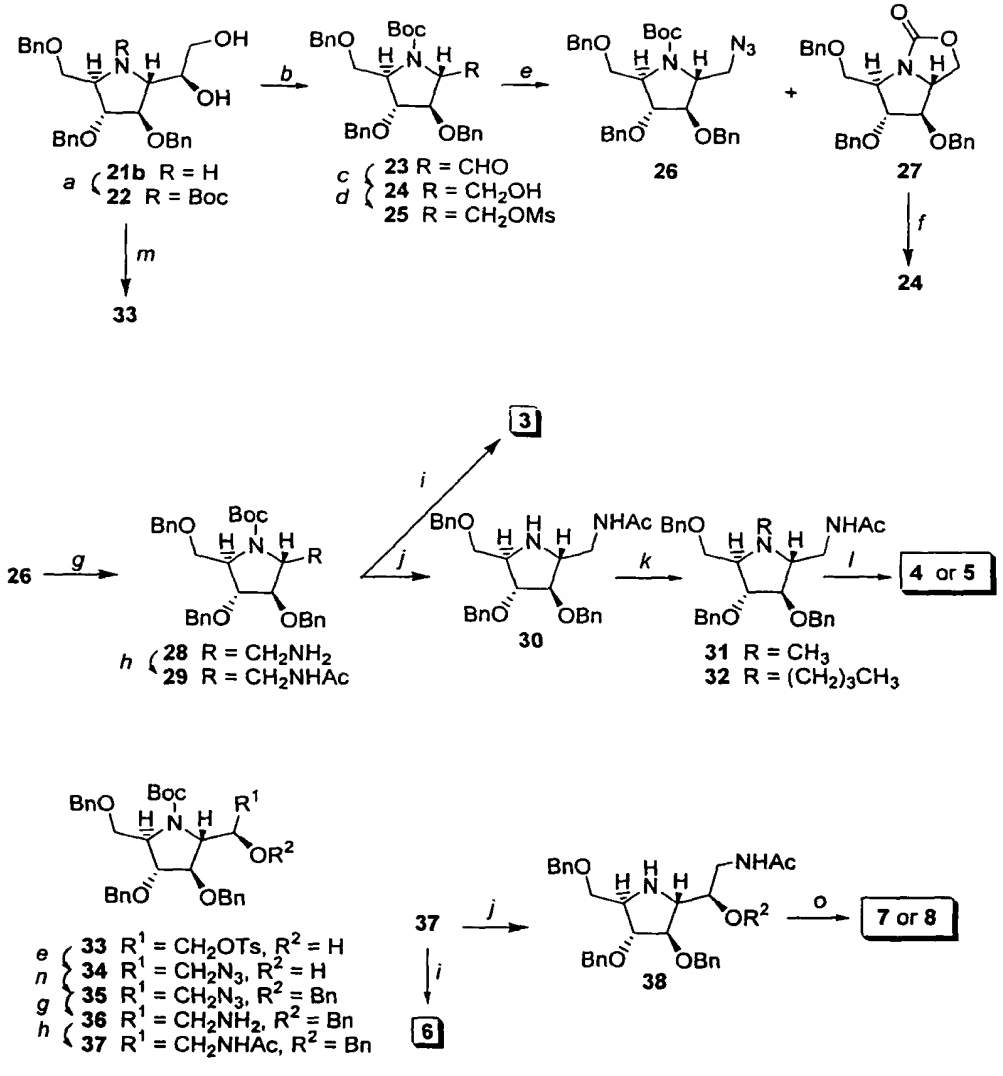


*a* $(Boc)_2O$ - $Et_3N$ / $CH_2Cl_2$; *b* $Pb(OAc)_4$ / toluene; *c* DIBAL / $CH_2Cl_2$; *d* MsCl - $Et_3N$ / $CH_2Cl_2$; *e* $NaN_3$ / DMF; *f* 1) $LiAlH_4$ / THF, 2) $(Boc)_2O$ - $Et_3N$ / $CH_2Cl_2$; *g* $H_2$ - Pd/C / MeOH; *h* $Ac_2O$ - Pyr.; *i* 1) $H_2$ - Pd/C / MeOH - HCl, 2) TFA; *j* TFA; *k* $CH_2O$ or $CH_3(CH_2)_2CHO$ - $NaBH_3CN$ / MeOH; *l* $H_2$ - Pd/C / MeOH - HCl; *m* TsCl - Pyr.; *n* BnBr - $Ag_2O$ - KI / DMF; *o* 1) $CH_2O$ or $CH_3CHO$ - $NaBH_3CN$ / MeOH, 2) $H_2$ - Pd/C / MeOH - HCl.

FIG. 6

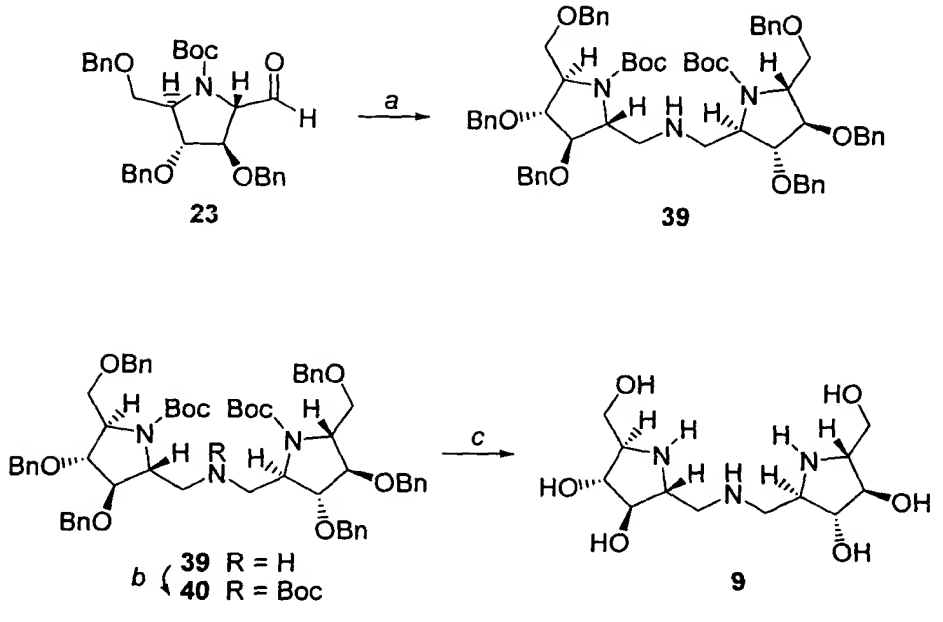


*a* $NH_4OAc$ - $NaBH_3CN$ / MeOH; *b* $(Boc)_2O$ - $Et_3N$ / $CH_2Cl_2$; *c* 1) Pd/C / MeOH - HCl, 2) TFA.

FIG. 7

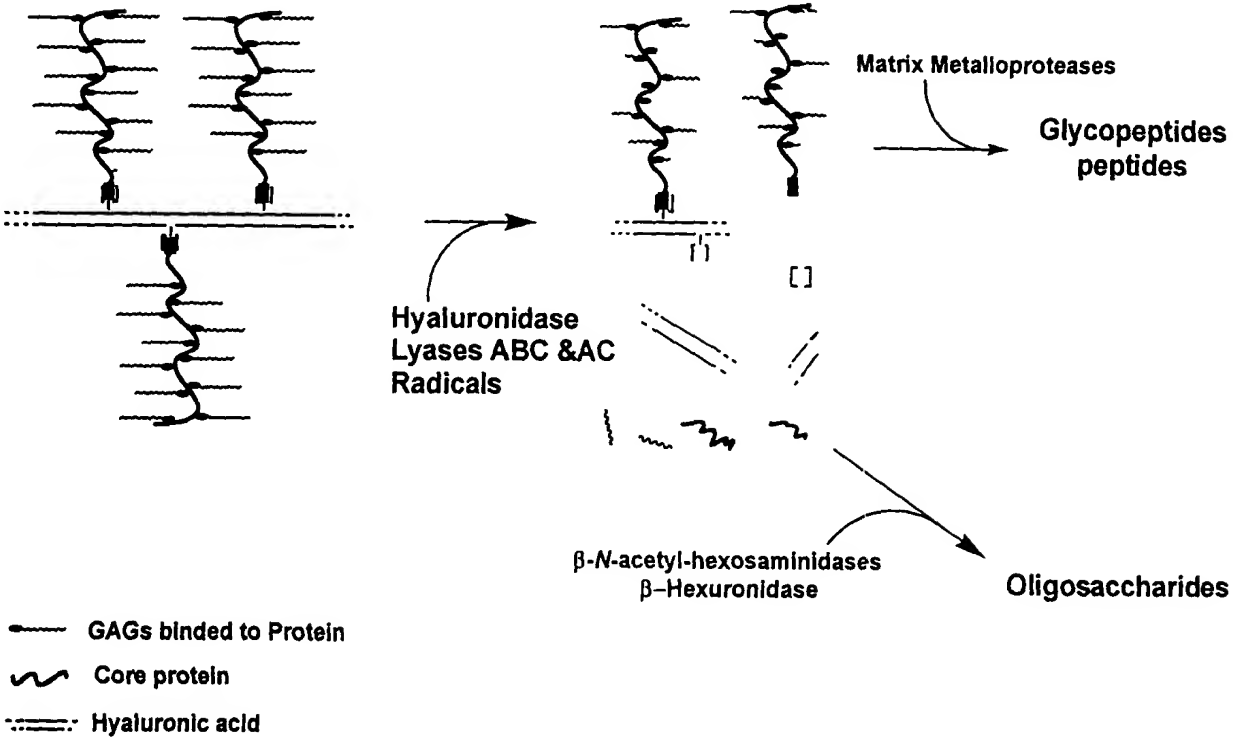


FIG. 8

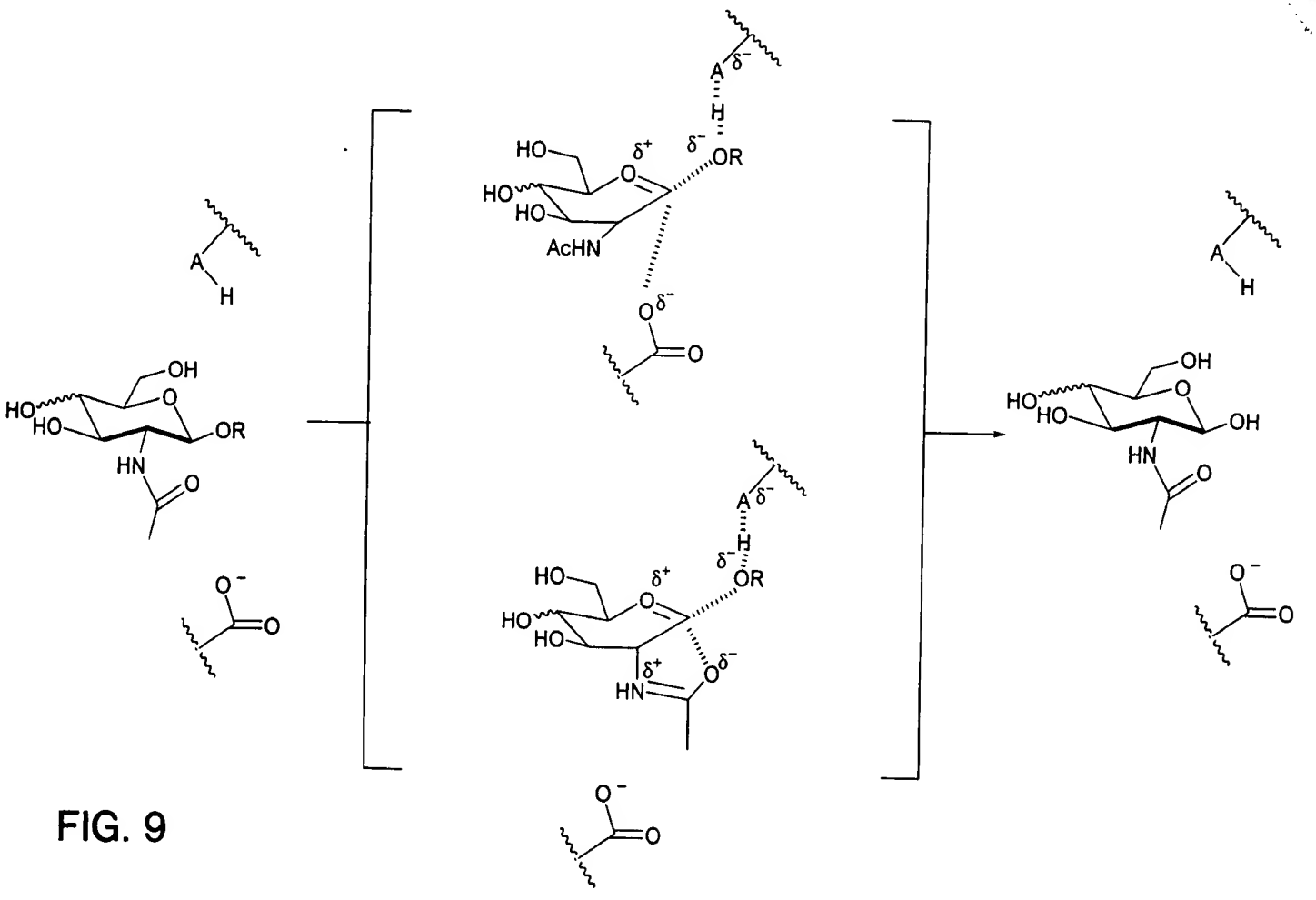


FIG. 9

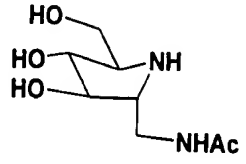


3

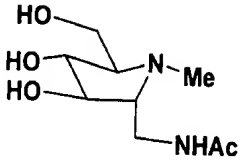


4

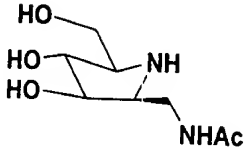


103

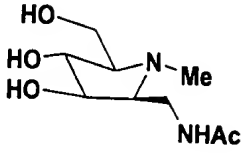


104

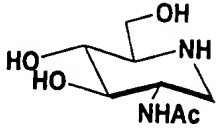


105

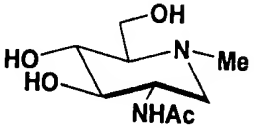


106

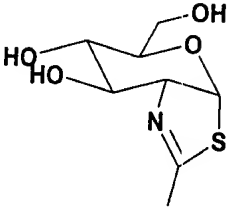


107

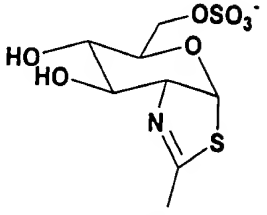


108

FIG. 10

| | 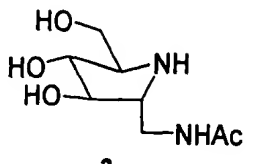 3 | 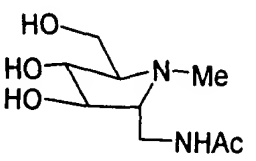 4 | 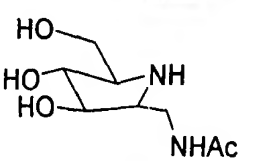 103 | 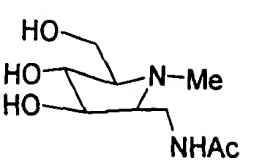 104 |
|---|---|---|---|---|
| Ki | — | 24nM | — | — |

| | 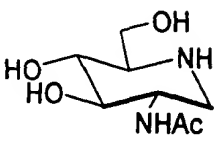 105 | 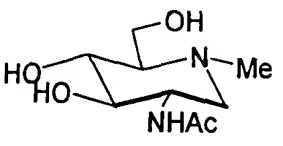 106 | 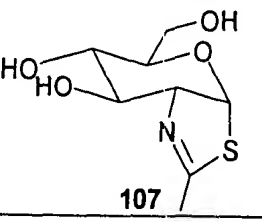 107 | 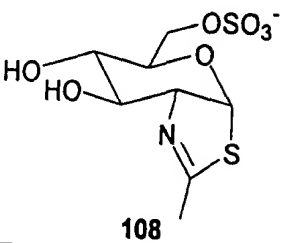 108 |
|---|---|---|---|---|
| Ki | 1200nM | 860nM | $IC_{50}MUG<IC_{50}MUGS$ ~ 10μm | $IC_{50}MUG=100\mu m$ $IC_{50}MUGS<10\mu m$ |

— Not assayed yet

FIG. 11

EFFECT OF SELECTED HEXOSAMINIDASE INHIBITORS ON INTRACELLULAR HEXOSAMINIDASE ACTIVITY

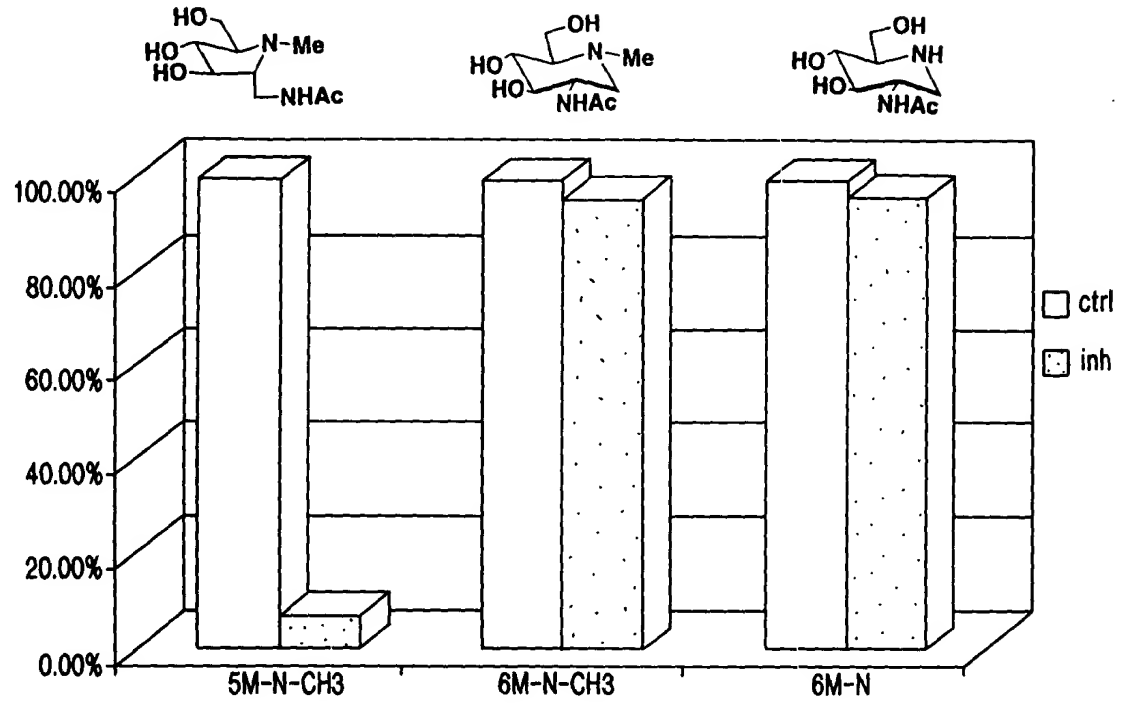


FIG. 12

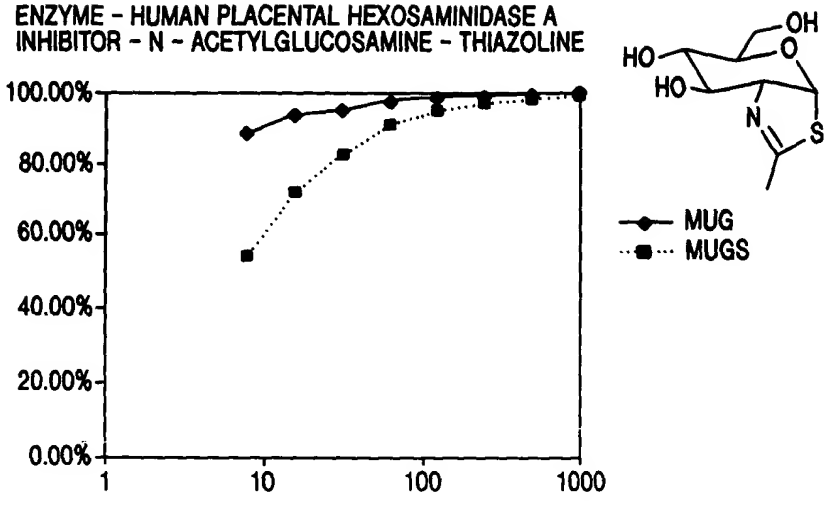


FIG. 13A

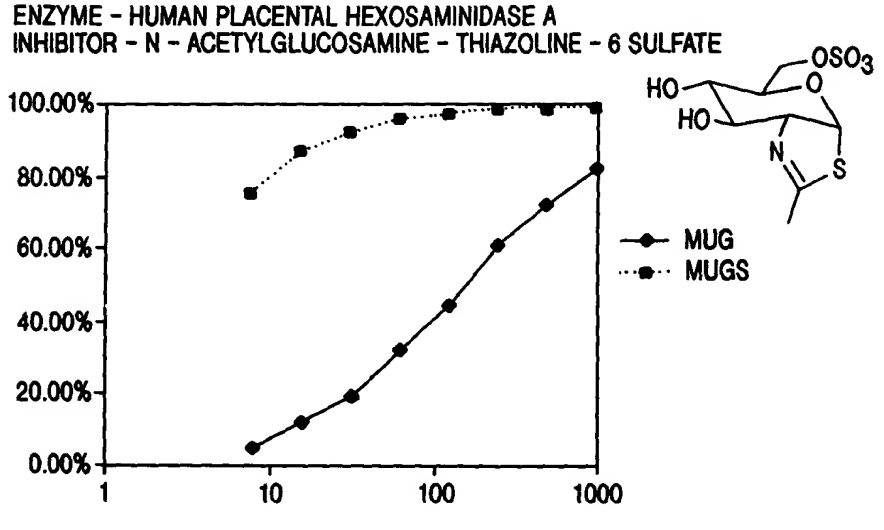


FIG. 13B

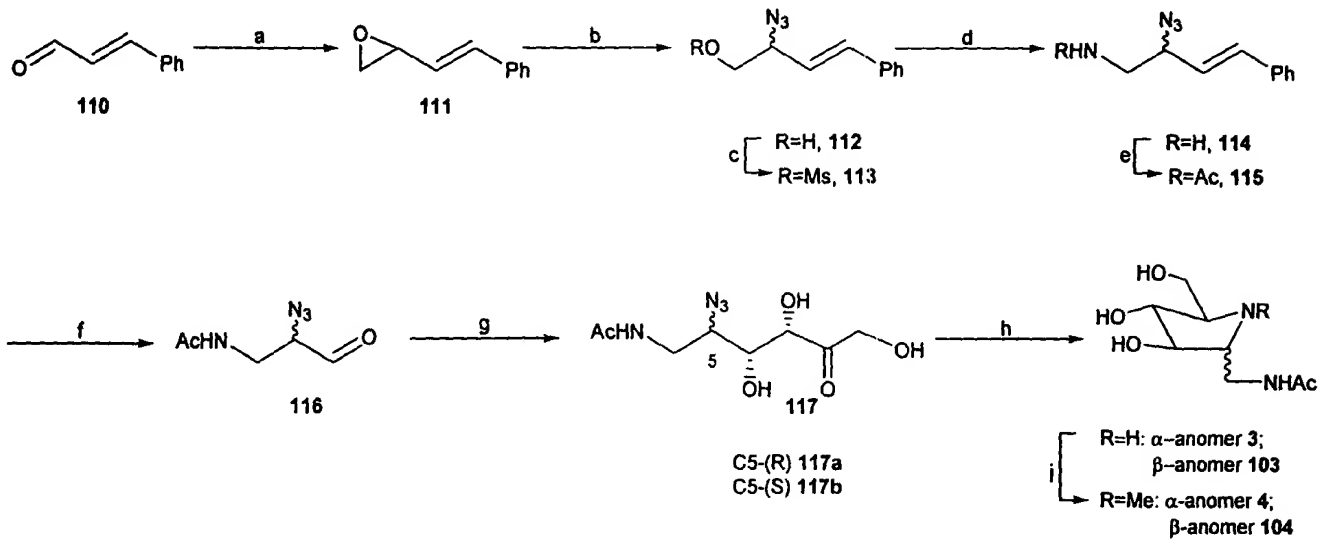


a. $Me_3S^+I$/NaH, DMSO/THF; b. $NaN_3$, acetone/$H_2O$, 82% from **110**: c. MsCl, Pyr. 96%; d. HMTA, NaI/EtOH; HCl, 65°C; e. isopropenyl acetate, 85% from **113**; f. $O_3$, $Me_2S$; g. DHAP, RAMA, pH=6.5; acid pase 37°C, pH=4.7; 44% for (R), 30% for (S); h. Pd-C/$H_2$, 80%; i. $CH_2O$, Pd-C/$H_2$, 90%.

FIG. 14

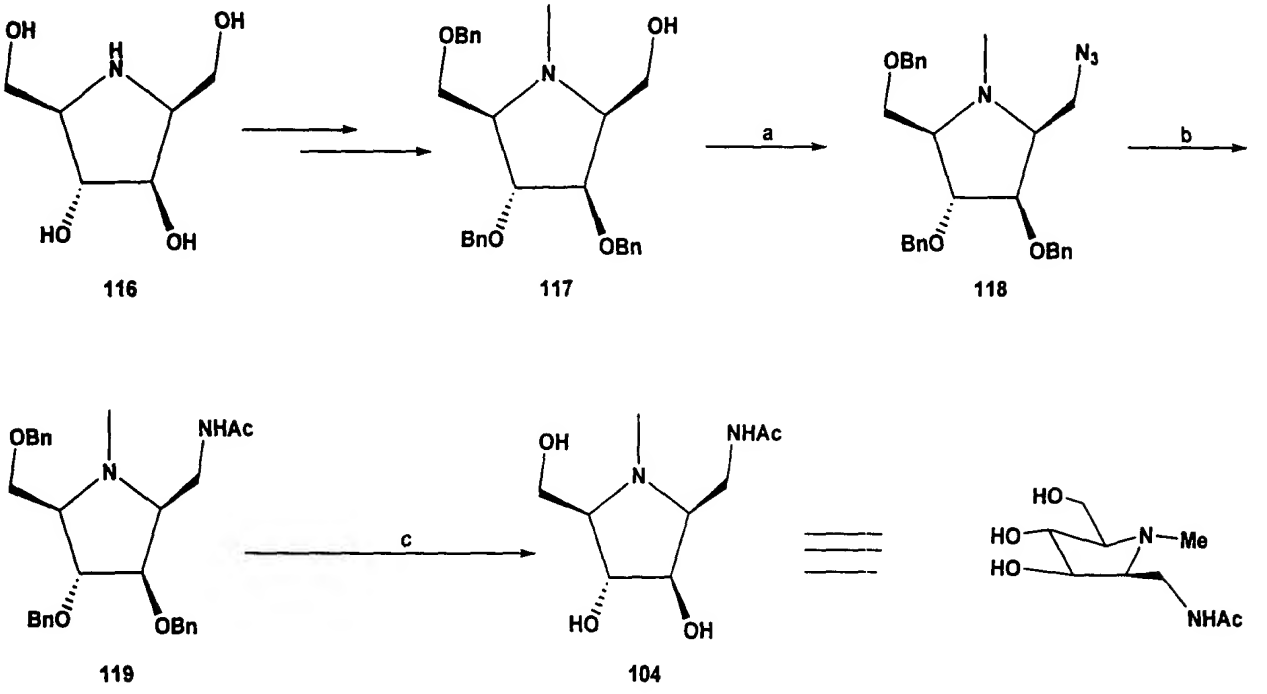


a. MsCl, Pyr; $NaN_3$, $CH_2Cl_2$, 87% for 2 steps; b. $PPh_3$, THF; $Ac_2O$, Pyr. 87% from 118; c. Pd-C/$H_2$ 50 psi, 89%.

FIG. 15

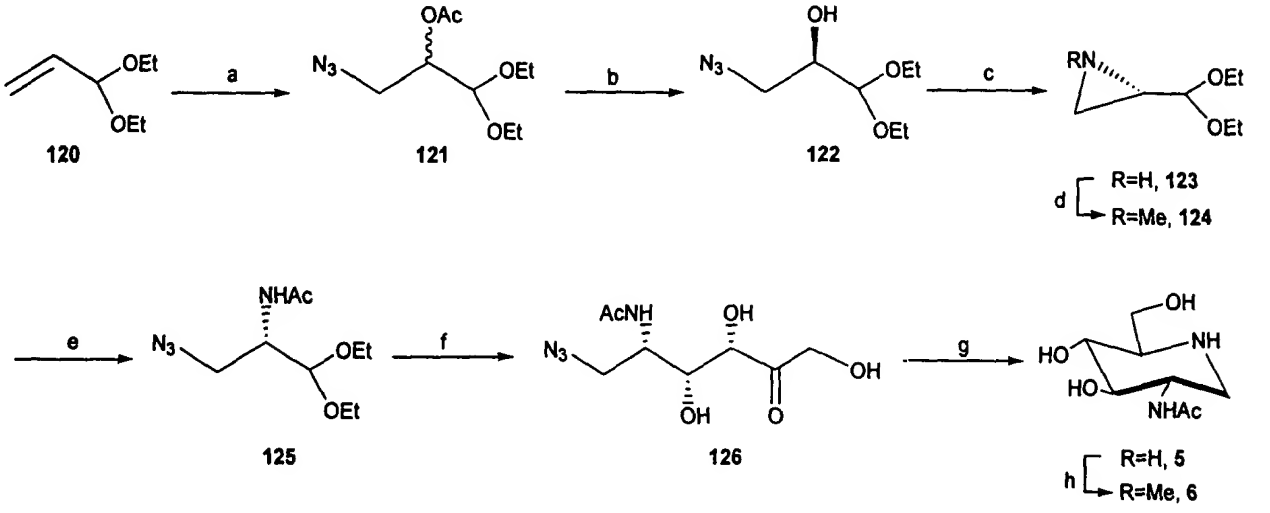


a. $H_2O_2$, PhCN; $NaN_3$, pH=7.5; $Ac_2O$, Pyr. 76% for 3 steps; b. PS-80, pH=7.0, 45%, 98%ee; c. $Ph_3P$, toluene, 120°C; d. $Ac_2O$, $K_2CO_3$, 30% for 2 steps; e. $NaN_3$, $ZnCl_2/Et_2O$, DMF 75°C, 62%; f. pH=1, 45°C; DHAP, RAMA, pH=6.5; pH=4.7, acid pase, 37°C, 55% for 3 steps; g. Pd-C/$H_2$, 87%; $CH_2O$, Pd-C/$H_2$, 92%.

FIG. 16

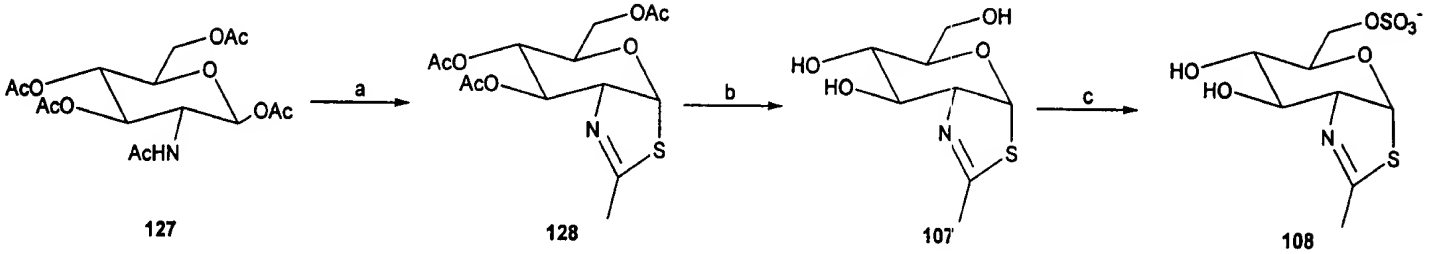


127 128 107 108

a. Lawesson's reagent, toluene, 80°C; b. MeONa/MeOH, 85% for 2 steps; c. $SO_3{\cdot}NMe_3$, Pyr. 0°C, 87%.

FIG. 17

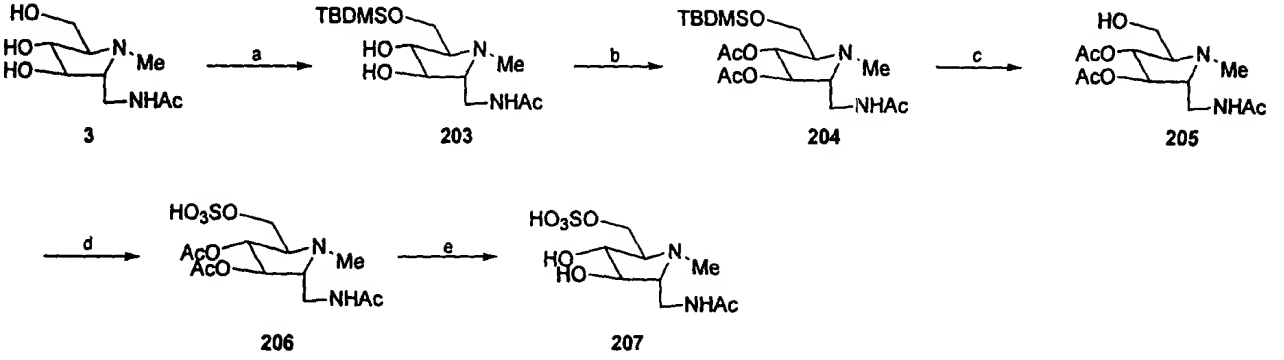


a. TBDMSCl, TEA, 0°C, DMF, overnight, 88%; b. $Ac_2O$, Pyridine, 0°C-rt. ; c. AcOH/$H_2O$/THF(5:1:3), 50°C. overnight, 75% for two steps; d. $SO_3$/Pyr, pyridine, 25 °C. 82%; e. cat. MeONa, MeOH, 85%

FIG. 18

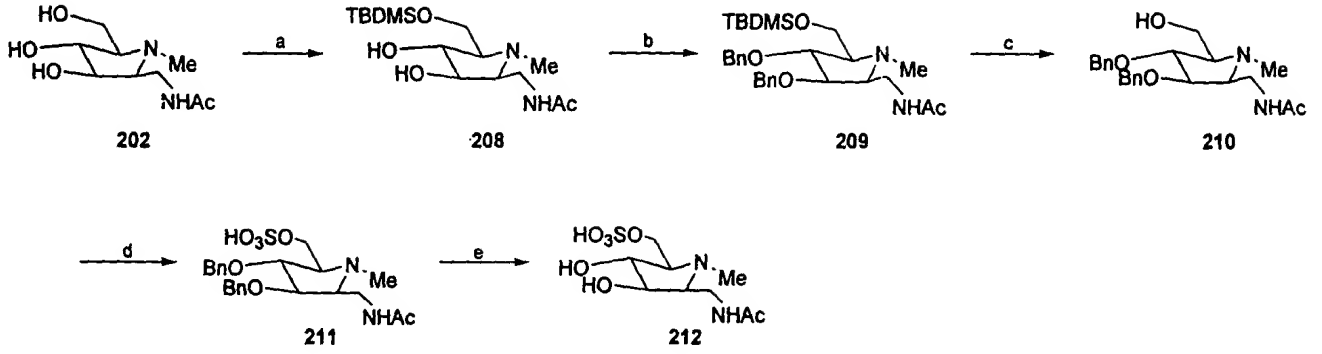


a. TBDMSOTf, TEA, 0 °C, DMF, 1.0 h, 90%; b. BnBr, NaH, 0 °C - 25 °C, 90%; c. TBAF, THF, 0 °C - 25 °C, 4h, 80%; d. $SO_3$/Pyr, pyridine, 25 °C, 80%; e. $Pd(OH)_2/C$, $H_2$, 75%

FIG. 19

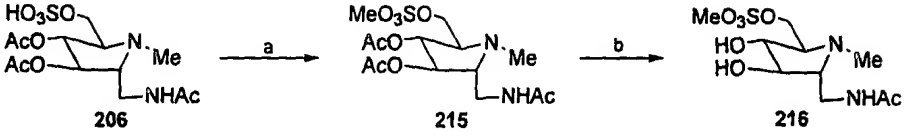


a. MeOH, 50°C, 1h, 90%; b. MeONa (cat.), MeOH, 3h, 80%.

FIG. 20